



Quantitative metrics for drug–target ligandability

Sinisa Vukovic¹ and David J. Huggins^{1,2}

¹ Department of Physics, Cavendish Laboratory, University of Cambridge, 19 JJ Thomson Avenue, Cambridge CB3 0HE, UK

² Department of Chemistry, University of Cambridge, Lensfield Road, Cambridge CB2 1EW, UK

Ligandability is a prerequisite for druggability and is a much easier concept to understand, model and predict because it does not depend on the complex pharmacodynamic and pharmacokinetic mechanisms in the human body. In this review, we consider a metric for quantifying ligandability from experimental data. We discuss ligandability in terms of the balance between effort and reward. The metric is evaluated for a standard set of well-studied drug targets – some traditionally considered to be ligandable and some regarded as difficult. We suggest that this metric should be used to systematically improve computational predictions of ligandability, which can then be applied to novel drug targets to predict their tractability.

Introduction

The druggability of a protein target is defined as the relative ease or difficulty of developing a small molecule that can effectively modulate protein activity *in vivo* [1]. The ligandability of a protein is defined as the relative ease or difficulty of developing a small molecule that can bind to the protein *in vitro* [2]. This is an important difference, because there are many complex pharmacokinetic and pharmacodynamic (PKPD) factors that influence druggability but not ligandability [3,4]. This makes ligandability a prerequisite for druggability and an easier concept to measure and predict. Consequently, there are many computational methods for predicting drug–target ligandability. All of these rely on a structural characterisation of the target [5,6]. Before making a prediction of ligandability it is necessary to identify the particular binding site of interest. When the target is structurally characterised, the relevant binding site tends to be known. However, the biologically relevant binding site might not be known and/or there might be an interest in identifying additional allosteric sites [7]. In these cases, there are several computational methods for predicting binding sites. Structure-based predictive methods include LIGSITE [8], PocketDepth [9], Fpocket [10], Q-SiteFinder [11] and i-Site [12]. Once the relevant region(s) of the target has been

identified, one of the several computational approaches can be used to predict the druggability or ligandability of the target. These include MAP_{POD} [13], SiteMap [14], WaterMap [15], fpocket [16], DLID [17], DrugFEATURE [18], DrugPred [19], FTMap [20], JEDI [21] and others [22,23]. It is worth noting that some methods, such as MAP_{POD} and SiteMap, deliberately aim to capture features of the binding site that will bind drug-like molecules.

Several experimental metrics for ligandability have been proposed. The first class of metric is based on experimental screening hit-rates. This idea was introduced by Hajduk *et al.* [4,24] who compared hit-rates from fragment screening with the existence of high-affinity ($K_d < 300$ nM), non-peptide, noncovalent inhibitors of the target. Taking this idea further, Edfeldt *et al.* combined fragment hit rates with the fragment affinities and the chemical diversity of the hits [2]. In recent times, ¹⁹F NMR has proven to be an important technique to rapidly assess a novel drug target using fragment hit rates [25,26]. However, there are two caveats in the use of the fragment hit rates alone to predict target ligandability. Firstly, it is not guaranteed that a high hit rate for fragment binding means that it will be easy to identify a small-molecule inhibitor with sufficient binding affinity. Many proteins have binding hotspots [27] that bind fragments with high affinity [24] but are challenging drug targets. A protein surface site with a small isolated pocket would be such an example. Even with two

Corresponding author: Huggins, D.J. (djh210@cam.ac.uk)

pockets that are disconnected by some distance it can be extremely challenging to grow or link the fragments to identify high-affinity druglike inhibitors [28]. This is particularly true for protein–protein interactions. Secondly, hit rates must be standardised and not depend on arbitrary thresholds, assay conditions or choice of fragment library. This makes selection of an appropriate fragment library very important [29]. Despite these caveats, fragment screening to assess target ligandability remains a very useful technique. The second class of metrics is based on similarity to other targets that are known to be tractable. However, even small differences in sequence can markedly alter ligand binding and thus this method can be highly inaccurate. The third metric is based on analysis of historical data for a target. There is an abundance of experimental data cataloguing measured protein–ligand binding affinities: PubChem [30], BindingDB [31], ChEMBL [32], Binding MOAD [33], PDBbind [34], AffinDB [35], ChemSpider [36] and others. One of the earliest papers on this topic suggested assessing ligandability using the idea of maximal affinity [13]. The idea is that high affinity ligands should have been developed for a highly ligandable target, whereas weaker affinity ligands should have been developed for a target with lower ligandability. This is a logical and effective idea, but there is a caveat. Consider two protein targets for which a similar binding affinity has been reached. If one of the targets requires the testing of ten-times as many ligands to achieve this binding affinity it is arguably a significantly less ligandable target. With this in mind, we attempt to address two important issues with current concepts of ligandability.

- The majority of studies make a binary distinction between druggable and undruggable targets. Ligandability and druggability are relative concepts, such that separating targets into druggable and undruggable will always be arbitrary. A continuous metric, such as the best-known affinity [13], is

more natural and more useful to inform decision making in drug design.

- One of the reasons that a binary distinction of ligandability has been favoured is that quantification of target ligandability is difficult. Visual inspection of data and personal experience of a given target are not ideal. Experimentally quantifying target ligandability requires careful and unbiased analysis of a large body of data.

We discuss an alternative to the concept of maximal affinity, proposing a continuous metric for ligandability based on experimental data. We present a concept of ligandability that is based on the binding affinity achieved for a target as well as the effort necessary to reach this binding affinity. We consider binding affinity data from BindingDB [31] expressed as K_i measurements. Figure 1 shows the pK_i values for ~20,000 compounds, plotted against the molecular weight. The distribution shows a similar picture to previous studies, with a very weak correlation of 0.33 and an apparent ceiling around $pK_i = 15$ (1 fM affinity) [37]. We set out with the goal of devising a metric that quantifies ligandability in terms of the balance of effort and reward. Deriving this metric provides us with experimental ligandability metrics for well-studied targets and allows us to assess our computational predictions of ligandability. We have recently developed a method to predict ligandability from the desolvation penalty required to displace the solvent molecules from the surface of proteins, allowing a ligand to bind [38]. Similar to other computational methods, this approach requires a high-resolution 3D structure of the target to function. In this paper, we discuss an application of the method to a standard set of proteins that exhibit a range of ligandability [4]. This allows us to validate the algorithm by comparing with the experimental metric and make systematic improvements in the future.

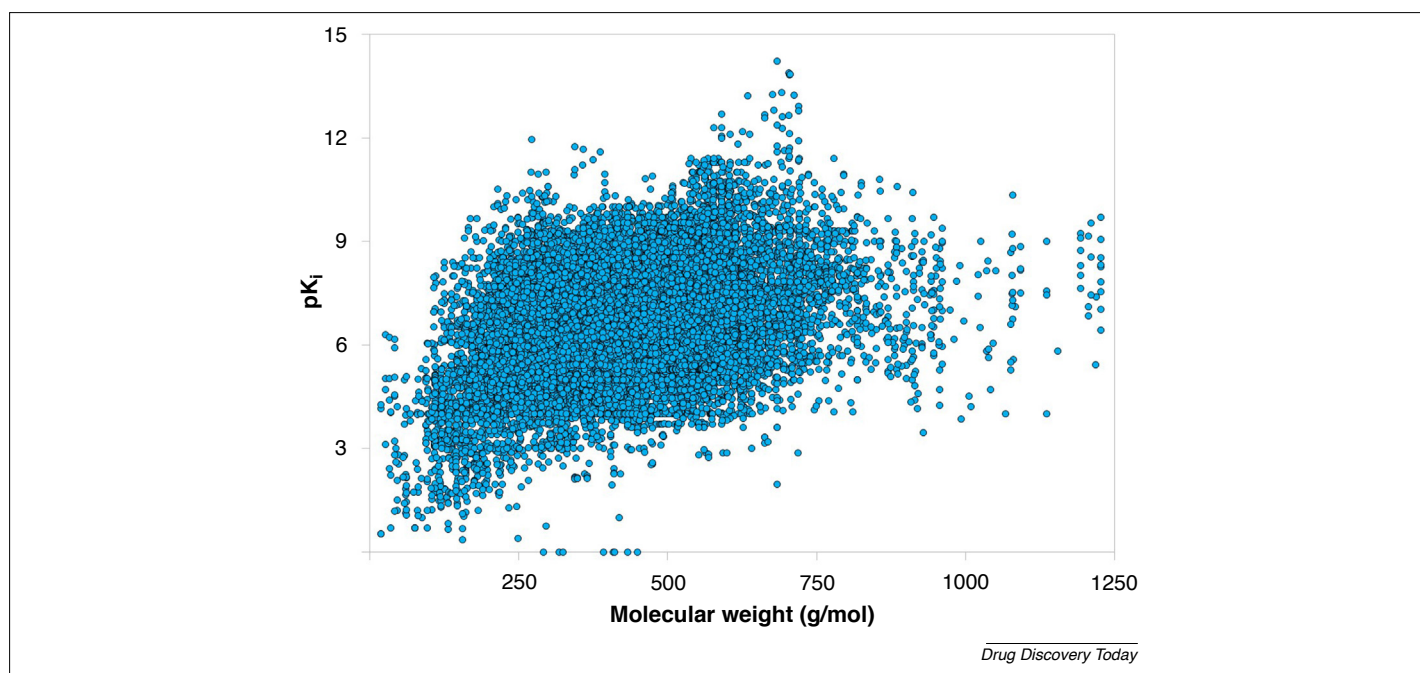


FIGURE 1

Binding affinity data as pK_i values plotted against molecular weight for 19,969 compounds from BindingDB [38] plotted as blue circles. The distribution shows a similar picture to previous studies, with a very weak correlation of 0.33 and an apparent ceiling around $pK_i = 15$ (1 fM affinity).

Ligandability metrics

The K_i data reported are from BindingDB. We begin by considering the maximal affinity measurements for a set of well-studied targets. Figure 2 shows pK_i -max for 442 targets along with the number of pK_i measurements for that target. The results show a very weak correlation between maximal affinity and the number of measurements ($R^2 = 0.11$), reinforcing the concept of differential ligandability. However, there is a notable difference between targets such as dihydrofolate reductase in red (maximal pK_i of 13.9 and 951 K_i measurements) and targets such as carbonic anhydrase I in blue (maximal pK_i of 11.0 and 5689 K_i measurements). It is instructive to consider the spread of pK_i values for a given target. Figure 3 shows the pK_i values in numerical order for 13 targets. If one equates the number of compounds tested with the effort expended, these data mean that some targets require significantly more effort to generate high affinity inhibitors than others. Taken together, the data suggest that maximal affinity alone is not sufficient to quantify ligandability. With this in mind, we set out to derive an alternative experimental measure of ligandability metric that captures the data presented in Fig. 3.

Experimental metrics for target ligandability

We consider a standard testset of 27 well-studied protein targets: 23 assigned as druggable and four as undruggable [13]. This set has been widely used in other studies [14–20]. The list of targets can be seen in Table 1. The metric for quantifying experimental ligandability (LIG_{exp}) was formulated on the concept of effort and reward: a target is highly ligandable if little effort is required to generate a high-affinity inhibitor. For the effort metric, we use the

total number of K_i values in BindingDB (N). The effort metric is a surrogate for the total monetary cost. We do not use IC_{50} or K_d values to maintain consistency, although this would provide significantly more data. For the reward metric, we use the number of reported compounds in BindingDB with a $pK_i > 7.0$. The reward metric attempts to characterise the broad achievement of high binding affinity. We then define LIG_{exp} as the proportion of compounds tested against a target with a $pK_i > 7.0$ (Eq. (1)).

$$LIG_{exp} = \frac{pK_i > 7}{N} \quad (1)$$

The metric is formulated such that a higher number represents a greater ligandability. A threshold of 7.0 maximises the variance in LIG_{exp} and thus provides the best possible discrimination between targets (for further details, see supplementary material online). With an experimental metric for ligandability in place, we move on to test our computational predictions. It is important to note that this metric lacks reliability if there are insufficient data available on the target. This is the reason why we consider only targets where BindingDB reports >100 K_i values. We discarded targets with <100 datapoints, leaving 13 of the original 27 proteins in our testset. We should note that we included all the experimental data in BindingDB for a given target, regardless of the physical properties. Thus, the data include compounds that might not be considered druglike. However, Fig. 1 demonstrates that the inclusion of compounds with a molecular weight >500 Da is unlikely to bias the pK_i distributions because increased molecular weight does not correlate with increased affinity above 500 Da. It is also worth noting that data for any target are inherently biased by the nature of the drug discovery goals of

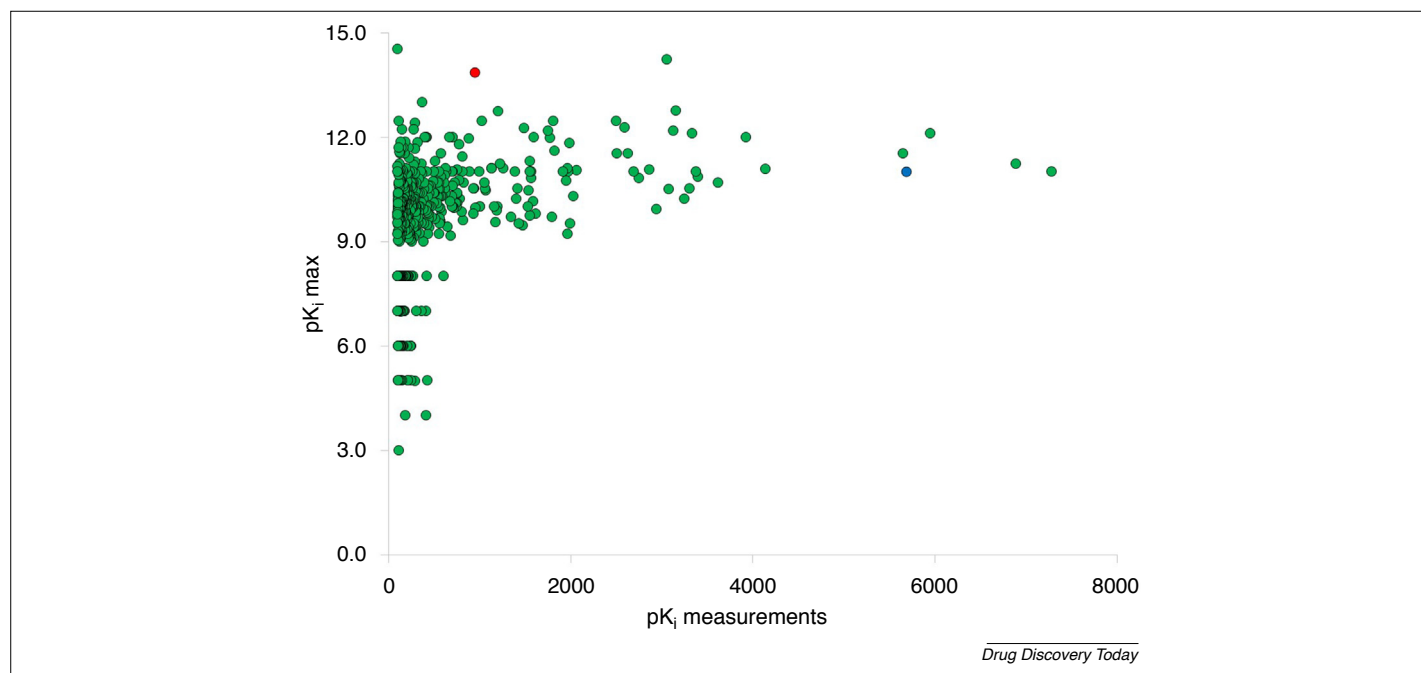
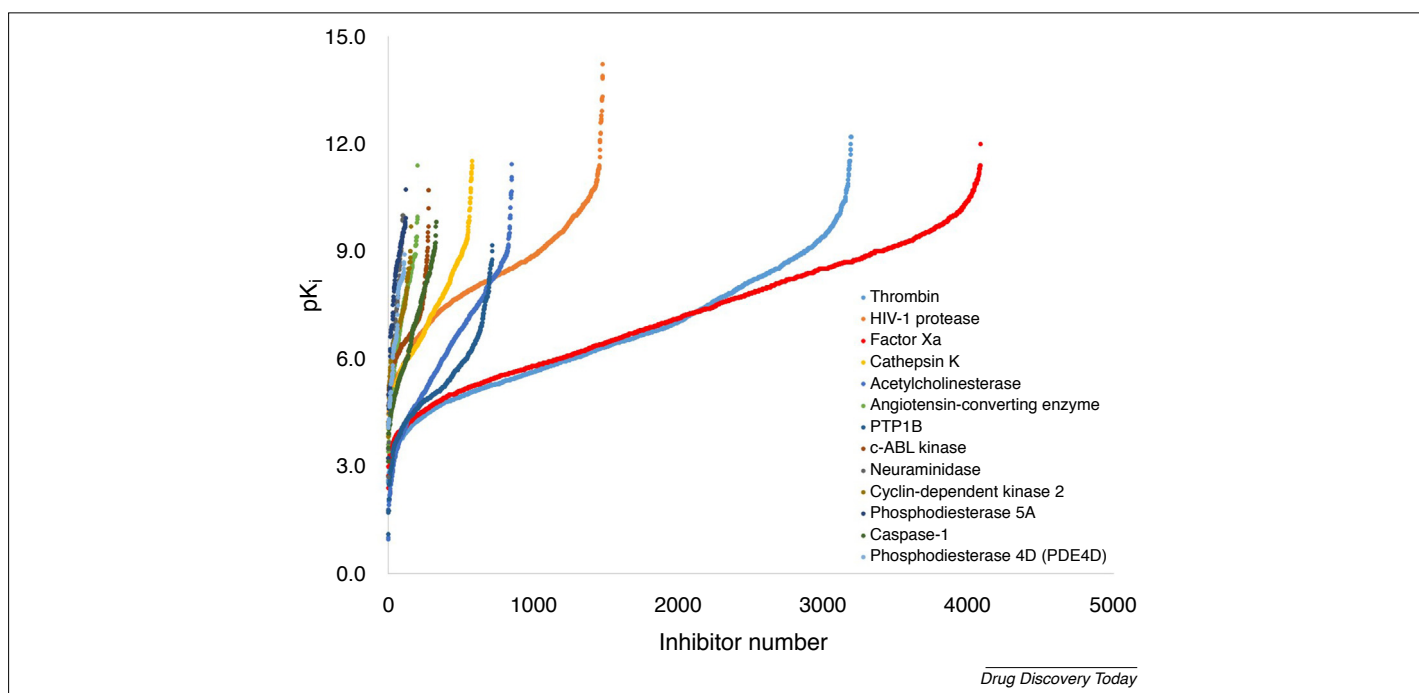


FIGURE 2

The total number of binding affinity datapoints (pK_i) plotted against the maximal pK_i for a set of 442 protein targets from BindingDB [38] plotted as green circles. The correlation is weak ($R^2 = 0.11$) reinforcing the concept of differential ligandability. For example, dihydrofolate reductase has high maximal pK_i for small effort (red circle) whereas carbonic anhydrase I has lower maximal pK_i even though much more effort has been put into finding a molecule with high pK_i (blue circle).


FIGURE 3

The distribution of pK_i values for 13 targets from BindingDB [38] plotted as multicoloured circles. The 13 targets are listed in the right-hand box and the datapoints for each target are coloured as shown. The data suggest that some targets require significantly more effort to generate high affinity inhibitors than others. In other words, maximal affinity alone is not sufficient to quantify ligandability.

the relevant projects. For example, later-stage projects are driven by other concepts such as selectivity or toxicology as well as affinity. In addition, some projects are aided by previous knowledge of the protein family, which can skew the distribution of reported affinities. An issue also arises owing to the difference between targets where just one lead series has been pursued (with a lot of analogues) and a target that has seen multiple lead series (with a smaller number of analogues per series). The former could have a range of affinities whereas the latter could have a large number of low-affinity hits. It is also highly likely that some of the data in BindingDB come from counter-screens against anti-targets. In particular, kinases, bromodomains, phosphodiesterases (PDEs) and cytochrome P450 are often used in counter-screens. However, we consider that using only well-studied targets should mitigate these problems to an acceptable degree. Finally, we point out that K_i values are somewhat arbitrary in nature given their dependence on assay conditions and in many cases by substrate concentrations. An analysis using average K_d values ($n > 3$) from biophysical binding assays would be more desirable, but such data are lacking in quantity and are still somewhat dependent on assay conditions.

Computational prediction of target ligandability

Although the concept of ligandability based on effort-and-reward is useful to distinguish among proteins that are already within the drug discovery pipeline, the lack of such data prevents us from doing the same for proteins that do not have reported K_i values. For such proteins, effective computational prediction of ligandability would be useful. We have reported such an approach in our previous work when we predicted the ligandability for apo structures of bromodomains and achieved reasonable agreement with

experimental data on available inhibitors [38]. This method of prediction is applied here as well. We use a computational method that is based on making an accurate estimation of the desolvation penalty that accompanies ligand binding. Water plays a vital part in small-molecule binding [39] and desolvation is one of the major determinants of binding affinity [40–42]. We calculate this desolvation penalty using a statistical mechanical method, based on molecular dynamics simulation of the protein in explicit water. We use the desolvation penalty as the computational prediction of ligandability (LIG_{comp}). This method is explained in detail in previous work [38]. For this reason, only a summary of the protocol is given below.

- **Stage 1.** Download the PDB file from the Protein Databank. Remove all co-solvents. Prepare the structure by adding hydrogen atoms, assigning protonation states and optimising the H-bond network using Schrodinger's PrepWizard.
- **Stage 2.** Place the protein in a periodic box of water molecules, such that the protein is at least 10 Å from the edge of the box on all sides. Neutralise the periodic box with chloride or sodium ions.
- **Stage 3.** Assign CHARMM27 [43,44] atom types and charges to the protein. Assign TIP4P-2005 [45] parameters to the water molecules.
- **Stage 4.** Restrain all protein heavy atoms harmonically with a force constant of 1.0 kcal/mol/Å².
- **Stage 5.** Equilibrate for 1.0 ns in the constant-pressure, constant-temperature (NPT) ensemble at 300 K.
- **Stage 6.** Simulate for 3.6 ns in the constant-pressure, constant-temperature (NPT) ensemble at 300 K.
- **Stage 7.** Cluster 1000 snapshots from the simulation to generate a set of hydration sites with a radius of 1.2 Å.

TABLE 1

The protein targets from Cheng's ligandability study. Data on the maximal reported pK_i were derived from the BindingDB [31]

Target	Total K_i measurements	Maximum pK_i
Factor Xa	3928	12.0
Thrombin	3129	12.2
HIV-1 protease	3055	14.2
Acetylcholinesterase	815	11.4
PTP1B	686	9.2
Cathepsin K	580	11.5
Caspase-1	332	9.8
c-ABL kinase	248	10.7
Angiotensin-converting enzyme	230	11.4
Phosphodiesterase 4D (PDE4D)	112	8.9
Cyclin-dependent kinase 2	105	9.7
Neuraminidase	103	10.0
Phosphodiesterase 5A	101	10.7
Cyclooxygenase-2 (COX-2)	98	8.3
IMPDH-II	95	8.2
IMPDH-I	92	9.0
Enoyl reductase	63	11.0
Aldose reductase (ALR2)	50	10.1
DNA gyrase subunit B	37	8.3
EGFR tyrosine kinase	21	9.5
MAP kinase p38	12	8.7
HIV-1 reverse transcriptase (NN)	12	7.5
Cytochrome P450 51	9	8.0
Mdm2-like p53-binding protein	3	7.7
HMG-CoA reductase	1	8.9
Hdm2	0	NA
HIV integrase	0	NA

Abbreviation: NA, not applicable.

- *Stage 8.* Calculate the binding affinity of waters in each hydration site using inhomogeneous fluid solvation theory [46] implemented in the Solvaware package [38].
- *Stage 9.* Calculate the summed binding affinity for every set of 18 connected hydration sites using the combinatorial subgraph search algorithm implemented in the Solvaware package. As shown previously, 18 hydration sites is approximately the size of a 500 Da inhibitor [38]. The displacement score for each cluster is the sum of the free energies of the constituent hydration sites.
- *Stage 10.* Identify the set of 18 connected hydration sites with the smallest displacement score. Record the displacement score and the location of the optimal binding site.

Clusters composed of weakly bound water molecules have a higher (less negative) displacement score and are predicted to yield highly ligandable hotspots. Comparison of the hotspots between proteins facilitates an assessment of relative ligandability. To ensure that the algorithm is focused on the binding site of interest, and not other regions of the protein, we only consider hydration sites within 20 Å of the known binding site (typically ~400–1000

TABLE 2

The displacement scores from the desolvation calculations and the predicted ligandability (LIG_{comp}) alongside the experimental ligandability metric from Eq. (1) (LIG_{exp}) for the 13 targets from Cheng's dataset with at least 100 K_i measurements

Target name	Displacement score (kcal/mol)	Predicted ligandability (LIG_{comp})	Experimental ligandability (LIG_{exp})
HIV-1 protease	−17.8	0.76	0.77
Phosphodiesterase 5A (PDE5A)	−17.7	0.77	0.75
Angiotensin-converting enzyme	−27.4	0.16	0.59
Factor Xa	−23.5	0.40	0.55
Cathepsin K	−21.2	0.55	0.53
Neuraminidase	−25.8	0.26	0.52
Cyclin-dependent kinase 2	−28.3	0.10	0.44
Caspase-1	−21.1	0.55	0.44
Phosphodiesterase 4D (PDE4D)	−19.7	0.65	0.42
Acetylcholinesterase	−21.5	0.53	0.37
Thrombin	−22.2	0.48	0.37
c-ABL	−21.7	0.51	0.33
PTP1B	−26.0	0.24	0.1
Minimum	−28.3	0.77	0.77
Maximum	−17.7	0.10	0.10

sites). To correspond to the values of the experimental metric for the targets studied (LIG_{exp}), the displacement scores are then scaled to the range 0.10–0.77.

Comparison of experimental and predicted ligandability

The ligandability metric (LIG_{exp}) has been computed for the 442 targets with >100 K_i values. Targets such as PDE10A (0.974), serine/threonine protein kinase PIM-1 (0.928) and angiotensin II receptor (0.856) are assigned high ligandability whereas targets such as β -lactamase Ampc (0.085), carbonic anhydrase III (0.009) and thymidylate kinase (0.000) are assigned low ligandability. All 442 ligandability values are shown in Table S1 (see supplementary material online). The correlation between LIG_{exp} values and the maximal pK_i values is 0.53. This suggests that there is a relationship between the maximal affinity and the spread of affinities, as might be expected. Importantly, the correlation between the experimental ligandability (LIG_{exp}) and the number of inhibitors tested is 0.11. This compares with a correlation of 0.33 between the maximal affinity and the number of inhibitors tested. Although a good ligandability metric should not show

TABLE 3

The druggability/ligandability predictions for the 13 targets from Cheng's dataset with at least 100 K_i measurements using Solvaware, MAP_{POD}, WaterMap and FTMap

Target name	LIG _{exp}	Solvaware (this work)	MAP _{POD} (nM)	SiteMap	FTMap
HIV-1 protease	0.77	0.76	0.66	1.06	D
Phosphodiesterase 5A (PDE5A)	0.75	0.77	0.029	1.15	D
Angiotensin-converting enzyme	0.59	0.16	130	1.00	D
Factor Xa	0.55	0.4	61	1.07	D*L
Cathepsin K	0.53	0.55	150	0.77	D
Neuraminidase	0.52	0.26	2100	0.90	D
Cyclin-dependent kinase 2	0.44	0.1	0.32	1.07	D
Caspase-1	0.44	0.55	540	0.86	B*S
Phosphodiesterase 4D (PDE4D)	0.42	0.65	0.29	1.04	D
Acetylcholinesterase	0.37	0.53	0.53	1.16	D
Thrombin	0.37	0.48	5.3	1.10	D
c-ABL	0.33	0.51	0.01	1.14	D
PTP1B	0.1	0.24	640	0.62	D

MAP_{POD} scores predict the maximal ligand affinity in nM, with a smaller score meaning higher druggability. The SiteMap predictions are the average DScore for each target, with a higher score indicating greater ligandability. The FTMap predictions are denoted as D (druggable using druglike compounds), D*L (druggable only by large chemotype such as macrocycle or foldamer), and B*S (micromolar affinity by peptide, macrocycle, or charged compound).

bias in over-scoring well-studied targets, one could argue that ligandable targets will be overrepresented in well-studied targets as projects on less ligandable targets could be discontinued early. We then moved on to assess the effectiveness of the computational predictions. Table 2 shows LIG_{exp} and LIG_{comp} for the 13 targets in the testset. The computational predictions show the correct trend, with a correlation of 0.42. The targets angiotensin-converting enzyme, neuraminidase and cyclin-dependent kinase 2 are relatively poorly predicted. All three are predicted to have low ligandability, but the experimental data suggest that they have intermediate ligandability. It is difficult to identify exactly why these poor predictions arise. However, in the case of angiotensin-converting enzyme, it seems likely that the method fails because of the presence of a very polar but ligandable pocket. The majority of inhibitors are charged and bind to the catalytic zinc ion, but the method prioritises hydrophobic sites with a low desolvation penalty. Notably, neuraminidase also contains a very polar pocket and binds predominantly to charged inhibitors. This should be addressed in any future releases of the software. For comparison, we have calculated the druggability and/or ligandability for these targets using MAP_{POD}, SiteMap and FTMap (Table 3). Predictions are hard to compare owing to different formats of prediction. However, it is clear that all methods do well for the highly ligandable targets HIV-1 protease and PDE5A. Conversely, FTMap correctly predicts angiotensin-converting enzyme as druggable when Solvaware and MAP_{POD} and SiteMap predict a lower ligandability. However, FTMap predicts that all but two of the targets are druggable (including the least ligandable target PTP1B) and SiteMap predicts that acetylcholinesterase and c-ABL are highly ligandable whereas the data suggest that they are challenging. In summary, all of these prediction algorithms have successes and failures, but we suggest that the dataset presented here will allow systematic improvement of these and other computational methods.

Concluding remarks and discussion

Accurate prediction of ligandability would be a useful tool in drug discovery to prioritise among different drug targets at an early stage or identify additional binding pockets on an existing drug target. Although a prediction of druggability is more desirable than a prediction of ligandability, druggability predictions are confounded by multiple difficulties related to PKPD issues such as cellular location and tissue distribution. These extend way beyond the structural characteristics of the target and are impossible to capture with the computational approaches now available. Conversely, ligandability depends on the structural characteristics of the target and is significantly easier to measure experimentally and computationally. We have presented a new metric for drug–target ligandability which takes into account the effort that has been expended on each target in addition to the rewards gained. For a given target, the metric is calculated as the fraction of inhibitors tested that are above a specified affinity cut-off. We selected an affinity cut-off of 100 nM, which maximises the discrimination between targets. We suggest that this metric is more effective than previous metrics because it does not show bias in over-scoring well-studied targets. It is also a more robust metric with respect to data errors and experimental uncertainty because it does not depend on individual binding affinity measurements. One issue with this metric is that the number of compounds is not necessarily a direct measure of effort. For example, target A might have been approached carefully by making a few select compounds whereas target B could have been approached by screening a large library at low cost. Alternatively, the chemistry for inhibitors of target A might be more challenging and require more synthetic effort per final molecule. However, by selecting only well-studied targets with >100 K_i values, we attempted to mitigate these problems. To further bolster the data, we could use IC₅₀ values or K_d values. It would also be extremely useful to have access to internal data from

pharmaceutical companies. This information could be shared without risking intellectual property and could provide some very useful post-competitive data. We calculated the ligandability metric for 442 targets from BindingDB. We consider that the dataset of 442 targets might be too large for validation of computational methods. However, restriction to targets with at least 1000 K_i measurements yields a dataset of 54 targets with a range of ligandability metrics from 0.125 to 0.890. These targets are listed in Table 4 and could be used in future work as a benchmarking set for computational methods. Using only these large datasets mitigates some of the issues discussed above such as dependence on assay conditions, lack of diversity in the dataset and experimental uncertainty in the data. Given the importance

TABLE 4

The experimental ligandability metric from Eq. (1) (LIG_{exp}) for 54 targets from the BindingDB with at least 1000 K_i measurements

Target	Experimental ligandability (LIG_{exp})	pK_i values (N)
Trace amine-associated receptor 1 (taar1)	0.890	1531
Apoptosis regulator bcl-2	0.828	1600
Histamine receptor (h3)	0.824	3082
Glucocorticoid receptor	0.799	1002
Melatonin receptor	0.776	1493
HIV-1 protease	0.765	3055
Poly-ADP-ribose polymerase 1 (PARP1)	0.748	1164
Carbonic anhydrase XII	0.739	1998
Sigma opioid receptor	0.736	1567
Melanin-concentrating hormone receptor	0.731	1541
Nociceptin receptor	0.721	1054
DRD2	0.692	1388
α -Adrenergic receptor (1a and 1d)	0.688	1568
G-protein-coupled receptor 44	0.687	1002
5-Lipoxygenase/FLAP	0.678	1476
Corticotropin-releasing factor receptor 1	0.675	1346
Serotonin (5-HT) receptor	0.674	6889
Carbonic anhydrase IX	0.666	2942
Leukocyte elastase	0.659	1133
D(3) dopamine receptor	0.650	3621
Histamine h1 receptor	0.614	1422
Kappa opioid receptor	0.604	3333
5-Hydroxytryptamine receptor 2a (5-HT2a)	0.604	1972
μ -Type opioid receptor (μ)	0.597	2510
Carbonic anhydrase II	0.594	5949
D(4) dopamine receptor	0.584	1951
Sigma-1 receptor	0.580	1557
Serotonin transporter (sert)	0.579	2692
Cannabinoid receptor 2 (CB2)	0.577	3378
Adenosine receptor a2b	0.575	1616
Melanocortin receptor 4	0.556	2028

TABLE 4 (Continued)

Target	Experimental ligandability (LIG_{exp})	pK_i values (N)
Coagulation factor X	0.554	3928
Somatostatin receptor	0.549	1915
Histamine receptor (h4)	0.537	1071
Delta opioid receptor	0.521	1752
5-Hydroxytryptamine receptor 2c (5HT2c)	0.519	1552
Adrenergic receptor alpha	0.495	2862
Cannabinoid receptor 1 (CB1)	0.485	2498
Muscarinic acetylcholine receptor m2 and m4	0.485	1264
Carbonic anhydrase IV	0.475	1965
Dopamine d2 receptor	0.465	5652
Neuronal acetylcholine receptor	0.459	1224
Dopamine transporter (dat)	0.455	3246
Adenosine receptor a2a	0.448	4138
Orexin receptor 2	0.441	1586
Norepinephrine transporters (net)	0.403	1435
Trypsin	0.376	1988
Thrombin	0.375	3129
Dopamine d1 receptor	0.371	1198
Adenosine receptor a1	0.340	3305
Orexin receptor 1	0.321	1405
Carbonic anhydrase I	0.255	5689
Monoamine oxidase	0.195	1194
Voltage-gated potassium channel	0.125	1175

of appropriate target selection and the ability to make predictions on one or relatively few structures, we consider the expenditure of significant computational resource on prediction of drug–target ligandability to be a worthwhile expenditure.

To make predictions of ligandability, we used a computational method based on the thermodynamics of the water network at the protein surface. The concept is that a cluster of weakly bound water molecules represents a ligand-binding hotspot, where a small desolvation penalty can be paid before forming the protein–ligand interactions. The method employed makes quantitatively accurate predictions of solvation thermodynamics [47,48]. We have also used this approach to consider all hydration sites on the surface of a protein (typically 2000–4000 sites) [38]. This global search finds the region of the protein with the lowest desolvation energy. A global search is useful for proteins for which the binding site is not known and allows an early assessment of traditionally difficult targets to predict tractability [49,50]. It is important to state that analysis of hydration sites around a protein only looks at part of the story for small-molecule binding. The desolvation penalty for displacing a cluster of hydration sites is compensated by interactions that a ligand will create once inside the volume of displaced hydration sites. For this reason, hydration sites with strongly bound water molecules tend not to be predicted as hotspots. In future work, this method could be developed by incorporating co-solvents and fragment probes into the simulation to

explicitly consider the balance between protein–solvent and protein–ligand interactions. This type of approach has been taken with FTMMap [51], which instead of displacability of solvent molecules tests different molecular fragments against the entire surface of the protein to detect regions for the best binding. We have included the comparison of scores with FTMMap and with MAP_{POD} and WaterMap (see Table 3).

We tested the method on 13 targets from BindingDB, each with >100 *K_i* measurements. The correlation between the experimental and predicted ligandability was 0.42 and this suggests that the computational method could be used as a flag to identify particularly challenging targets. However, although these results are reasonable, there is significant room for improvement. Importantly, the quantitative experimental metric described here enables systematic improvement of computational methods and we recommend its adoption in assessing predictive tools. It is important to note that there is an additional factor that should be applied to drug–target assessment using concepts of ligandability and that is the binding affinity of the cognate binding partner. For two drug targets with equal ligandability, it will be easier to inhibit the target which has a weaker affinity for its cognate binding partner. For this reason, we suggest that drug–target assessment should be focused on inhibitability rather than ligandability. This could be achieved easily with a small number of *in vitro* measurements. It is likely to be many years before computational methods can make accurate predictions of drug–target ligandability. However, accurate predictions of drug–target ligandability and inhibitability are achievable and will help us to extend the druggable genome in an effective manner.

Conflicts of interest

References

- Hopkins, A.L. and Groom, C.R. (2002) The druggable genome. *Nat. Rev. Drug Discov.* 1, 727–730
- Edfeldt, F.N. *et al.* (2011) Fragment screening to predict druggability (ligandability) and lead discovery success. *Drug Discov. Today* 16, 284–287
- Overington, J.P. *et al.* (2006) How many drug targets are there? *Nat. Rev. Drug Discov.* 5, 993–996
- Hajduk, P.J. *et al.* (2005) Predicting protein druggability. *Drug Discov. Today* 10, 1675–1682
- Mason, J.S. *et al.* (2012) New insights from structural biology into the druggability of G protein-coupled receptors. *Trends Pharmacol. Sci.* 33, 249–260
- Vidler, L.R. *et al.* (2012) Druggability analysis and structural classification of bromodomain acetyl-lysine binding sites. *J. Med. Chem.* 55, 7346–7359
- Gunasekaran, K. *et al.* (2004) Is allostery an intrinsic property of all dynamic proteins? *Proteins Struct. Funct. Bioinform.* 57, 433–443
- Hendlich, M. *et al.* (1997) LIGSITE: automatic and efficient detection of potential small molecule-binding sites in proteins. *J. Mol. Graph. Model.* 15, 359–363
- Kalidas, Y. and Chandra, N. (2008) PocketDepth: a new depth based algorithm for identification of ligand binding sites in proteins. *J. Struct. Biol.* 161, 31–42
- Le Guilloux, V. *et al.* (2009) Fpocket: an open source platform for ligand pocket detection. *BMC Bioinform.* 10, 168
- Laurie, A.T. and Jackson, R.M. (2005) Q-SiteFinder: an energy-based method for the prediction of protein–ligand binding sites. *Bioinformatics* 21, 1908–1916
- Morita, M. *et al.* (2008) Highly accurate method for ligand-binding site prediction in unbound state (apo) protein structures. *Proteins Struct. Funct. Bioinform.* 73, 468–479
- Cheng, A.C. *et al.* (2007) Structure-based maximal affinity model predicts small-molecule druggability. *Nat. Biotechnol.* 25, 71–75
- Halgren, T.A. (2009) Identifying and characterizing binding sites and assessing druggability. *J. Chem. Inf. Model.* 49, 377–389
- Beuming, T. *et al.* (2012) Thermodynamic analysis of water molecules at the surface of proteins and applications to binding site prediction and characterization. *Proteins Struct. Funct. Bioinform.* 80, 871–883
- Schmidtke, P. and Barril, X. (2010) Understanding and predicting druggability. A high-throughput method for detection of drug binding sites. *J. Med. Chem.* 53, 5858–5867
- Sheridan, R.P. *et al.* (2010) Drug-like density: a method of quantifying the “bindability” of a protein target based on a very large set of pockets and drug-like ligands from the Protein Data Bank. *J. Chem. Inf. Model.* 50, 2029–2040
- Liu, T. and Altman, R. (2014) Identifying druggable targets by protein microenvironments matching: application to transcription factors. *CPT Pharmacomet. Syst. Pharmacol.* 3, e93
- Krasowski, A. *et al.* (2011) DrugPred: a structure-based approach to predict protein druggability developed using an extensive nonredundant data set. *J. Chem. Inf. Model.* 51, 2829–2842
- Kozakov, D. *et al.* (2015) New frontiers in druggability. *J. Med. Chem.* 58, 9063–9088
- Cuchillo, R. *et al.* (2015) A collective variable for the rapid exploration of protein druggability. *J. Chem. Theory Comput.* 11, 1292–1307
- Loving, K.A. *et al.* (2014) Structure-based druggability assessment of the mammalian structural proteome with inclusion of light protein flexibility. *PLoS Comput. Biol.* 10, e1003741
- Rathi, P.C. *et al.* (2017) Predicting “hot” and “warm” spots for fragment binding. *J. Med. Chem.* 60, 4036–4046
- Hajduk, P.J. *et al.* (2005) Druggability indices for protein targets derived from NMR-based screening data. *J. Med. Chem.* 48, 2518–2525
- Aretz, J. *et al.* (2016) Chemical fragment arrays for rapid druggability assessment. *Chem. Commun.* 52, 9067–9070
- Jordan, J.B. *et al.* (2012) Fragment based drug discovery: practical implementation based on ¹⁹F NMR spectroscopy. *J. Med. Chem.* 55, 678–687
- DeLano, W.L. (2002) Unraveling hot spots in binding interfaces: progress and challenges. *Curr. Opin. Struct. Biol.* 12, 14–20
- Ichihara, O. *et al.* (2011) Compound design by fragment-linking. *Mol. Inform.* 30, 298–306
- Chen, I.-J. and Hubbard, R.E. (2009) Lessons for fragment library design: analysis of output from multiple screening campaigns. *J. Comput. Aided Mol. Des.* 23, 603–620

The authors declare no competing financial interests.

Acknowledgements

We would like to thank Paul Brennan, John Skidmore, Alan Cheng, Andrew Henry, Ian Wall, Andrew Leach, Paul Leeson and John Overington for helpful comments and the Cambridge High Performance Computing Service and ARCHER UK National Supercomputing Services for technical support. Work in the D.J.H. laboratory was supported by the Medical Research Council under grant ML/L007266/1. Many of the calculations were performed using the ARCHER UK National Supercomputing Services and the Darwin Supercomputer of the University of Cambridge High Performance Computing Service (<http://www.hpc.cam.ac.uk/>) provided by Dell using Strategic Research Infrastructure Funding from the Higher Education Funding Council for England; and were funded by the EPSRC under grants EP/F032773/1 and EP/J017639/1. We also thank the UK High-End Computing consortia for Biomolecular Simulation (HEC-BioSim) for providing access to the ARCHER UK National Supercomputing Services under grant EP/L000253/1.

D.J.H. conceived of the study, D.J.H. and S.V. designed the study, S.V. performed the calculations, D.J.H. and S.V. wrote the paper.

Appendix A. Supplementary data

Supplementary data associated with this article can be found, in the online version, at <https://doi.org/10.1016/j.drudis.2018.02.015>.

- 30 Kim, S. *et al.* (2015) PubChem substance and compound databases. *Nucleic Acids Res.* 44, D1202–D1213
- 31 Liu, T. *et al.* (2007) BindingDB: a web-accessible database of experimentally determined protein–ligand binding affinities. *Nucleic Acids Res.* 35, D198–D201
- 32 Gaulton, A. *et al.* (2011) ChEMBL: a large-scale bioactivity database for drug discovery. *Nucleic Acids Res.* 40, D1100–D1107
- 33 Hu, L. *et al.* (2005) Binding MOAD (mother of all databases). *Proteins Struct. Funct. Bioinform.* 60, 333–340
- 34 Wang, R. *et al.* (2004) The PDBbind database: collection of binding affinities for protein–ligand complexes with known three-dimensional structures. *J. Med. Chem.* 47, 2977–2980
- 35 Block, P. *et al.* (2006) AffinDB: a freely accessible database of affinities for protein–ligand complexes from the PDB. *Nucleic Acids Res.* 34 (Suppl. 1), D522–D526
- 36 Pence, H.E. and Williams, A. (2010) ChemSpider: an online chemical information resource. *J. Chem. Educ.* 87, 1123–1124
- 37 Kuntz, I. *et al.* (1999) The maximal affinity of ligands. *Proc. Natl. Acad. Sci. U. S. A.* 96, 9997–10002
- 38 Vukovic, S. *et al.* (2016) Exploring the role of water in molecular recognition: predicting protein ligandability using a combinatorial search of surface hydration sites. *J. Phys. Condens. Matter* 28, 34007
- 39 Ringe, D. (1995) What makes a binding site a binding site? *Curr. Opin. Struct. Biol.* 5, 825–829
- 40 Gohlke, H. and Klebe, G. (2002) Approaches to the description and prediction of the binding affinity of small-molecule ligands to macromolecular receptors. *Angew. Chem. Int. Edn.* 41, 2644–2676
- 41 Mondal, J. *et al.* (2014) Role of desolvation in thermodynamics and kinetics of ligand binding to a kinase. *J. Chem. Theory Comput.* 10, 5696–5705
- 42 Mobley, D.L. and Dill, K.A. (2009) Binding of small-molecule ligands to proteins: “what you see” is not always “what you get”. *Structure* 17, 489–498
- 43 Mackerell, A.D. *et al.* (1998) All-atom empirical potential for molecular modeling and dynamics studies of proteins. *J. Phys. Chem. B* 102, 3586–3616
- 44 Mackerell, A.D. *et al.* (2004) Extending the treatment of backbone energetics in protein force fields: limitations of gas-phase quantum mechanics in reproducing protein conformational distributions in molecular dynamics simulations. *J. Comput. Chem.* 25, 1400–1415
- 45 Abascal, J.L.F. and Vega, C. (2005) A general purpose model for the condensed phases of water: TIP4P/2005. *J. Chem. Phys.* 123, 234505
- 46 Li, Z. and Lazaridis, T. (2003) Thermodynamic contributions of the ordered water molecule in HIV-1 protease. *J. Am. Chem. Soc.* 125, 6636–6637
- 47 Huggins, D.J. (2014) Estimating translational and orientational entropies using the *k*-Nearest Neighbors Algorithm. *J. Chem. Theory Comput.* 10, 3617–3625
- 48 Huggins, D.J. (2015) Quantifying the entropy of binding for water molecules in protein cavities by computing correlations. *Biophys. J.* 108, 928–936
- 49 Surade, S. and Blundell, T.L. (2012) Structural biology and drug discovery of difficult targets: the limits of ligandability. *Chem. Biol.* 19, 42–50
- 50 Laraia, L. *et al.* (2015) Overcoming chemical, biological, and computational challenges in the development of inhibitors targeting protein–protein interactions. *Chem. Biol.* 22, 689–703
- 51 Brenke, R. *et al.* (2009) Fragment-based identification of druggable ‘hot spots’ of proteins using Fourier domain correlation techniques. *Bioinformatics* 25, 621–627